九州大学学術情報リポジトリ
Kyushu University Institutional Repository

Surface Modification and Hardness Behavior of AISI 304 as an Artificial Hip Joint using Ammonia and Scallop Shell Powder as a Nitriding Agent

Triyono, Joko
Department of Mechanical Engineering Sebelas Maret University

Rahajeng, Raihan
Department of Mechanical Engineering Sebelas Maret University

Surojo, Eko
Department of Mechanical Engineering Sebelas Maret University

https://doi.org/10.5109/4480714

出版情報：Evergreen. 8 (2), pp.335-343, 2021-06. Interdisciplinary Graduate School of Engineering Sciences, Kyushu University, Japan
バージョン：
権利関係：Creative Commons Attribution-NonCommercial 4.0 International

KYUSHU UNIVERSITY

Surface Modification and Hardness Behavior of AISI 304 as an Artificial Hip Joint using Ammonia and Scallop Shell Powder as a Nitriding Agent

Joko Triyono[1,*], Raihan Rahajeng[1], Eko Surojo[1]
[1]Department of Mechanical Engineering Sebelas Maret University,
Surakarta, Central of Java, Indonesia

*Author to whom correspondence should be addressed:
E-mail: jokotriyono@staff.uns.ac.id

(Received November 17, 2020; Revised May 6, 2021; accepted June 4, 2021).

Abstract: Surface modification was carried out in AISI 304 using ammonia and scallop shell powder as the nitriding agent. Furthermore, the temperature variations used were 500°, 550° and 600°C within the durations of 3, 5, and 7 hours. The results showed that the highest point of specimen hardness reached 600°C at 7 hours (1246 VHN) with a nitrogen content of 15.35% and a nitride layer depth of 141.64 µm. In addition, this value was higher than other implant materials, namely AISI 316L (316 VHN), Ti6Al4V (435 VHN), CrCoMo (351 VHN) and human bone (129 VHN).

Keywords: surface modification, hardness, AISI 304, hip joint, ammonia, scallop shell.

1. Introduction

An implant prosthetic material is used in replacing a damaged hip joint due to osteoarthritis, rheumatoid arthritis, fractures, cancer, or other factors[1)]. Therefore, total hip replacement is a medical procedure aimed at replacing the damaged part of the hip with an artificial hip joint. The acetabulum and femoral head are replaced with a prosthetic device[2)]. Furthermore, this process has the highest success rate for treating osteoarthritis or severe hip rheumatoid arthritis patients[3)]. Metal is the main alternative in the choice of prosthetic material because of its superior mechanical properties.

Therefore, the prosthetic joint implant material needs to have several requirements[4)], namely adequate pain relief function, capability to correct deformities, endurance, satisfactory salvage potential, chemical inertness, sterility, and appropriate fit. The hip prosthesis material needs to also have an insignificant coefficient of friction, high surface hardness, scratch resistance, and the ability to produce minimal debris. In addition, any implant surface exposed to human tissue needs to be non-cytotoxic, biocompatible, and bioinert[5)].

Prosthetic materials used mainly for hip joints are stainless steel, Co-Cr alloys, and Ti alloys[6)]. Stainless steel is commonly used because of its hygiene, corrosion resistance, and workmanship[7)], and the series used is AISI 316L[8)]. Furthermore, other materials used as hip prosthetic materials include AISI 304 and Ti-alloy[9-11)]. For hip joint prosthesis, stainless steel has several disadvantages such as hardness and wear resistance which is insufficient for extended use[12)] and lacks the stability to withstand dynamic loads in aggressive environments[13-14)]. Therefore, surface modification is needed to overcome these drawbacks. Properties of cell adhesion, differentiation, non-cytotoxicity, and osteoconductivity also need to be considered before carrying out surface modification treatment[15)].

This study aims to analyze the change of AISI 304 steel surface properties before and after the nitriding process. Furthermore, the nitriding agent used consists of ammonia and shell powder mixture. It was used to form an N-rich hardened layer containing the precipitated austenite/S-phase and expanded CrN-Cr_2N. The shells were extracted by deproteination and demineralization using two bacteria strains sequentially[16-17)]. Furthermore, since ammonia and shell powder are easily found in Indonesia, this method is famous for its simplicity and frugality[18)].

Austenitic stainless steels containing S-phase have some advantages as biomaterials. According to the medical standpoint, they include hardness, wearability, and corrosion resistance[19)]. This study described the significant increase in the hardness of AISI 304 material after surface modification.

2. Methods

This research was carried out in four stages, namely specimen preparation, pack nitriding treatment, micro Vickers hardness test, and SEM-EDS observation.

2.1 Preparation of specimen

AISI 304 stainless steel round bar was cut into short cylinders of 13mm diameter and 20mm height according to ASTM E384-17[20], as shown in Fig. 1.

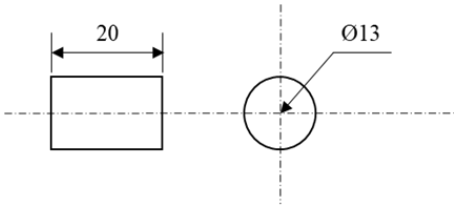

Fig.1: Initial dimensions of the specimen in milimeter

The top surface of the specimen was sanded on 200, 320, 400, 600, 800, 1000, and 1,200 grit abrasive paper. Furthermore, it was polished using diamond paste, and cleaned of dirt and grease.

Fig. 2: Terracotta bowl used as nitriding vessel inside the electric furnace

2.2 Pack nitriding treatment

The nitriding agent used was the mixture of ammonia and scallop shell powder in the ratio of 2:3 (%wt). Specimens had been placed distantly from each other in the middle of terracotta bowl filled with the nitriding agent. Furthermore, the top of the bowl was covered by aluminum foil and was tightly closed. The position of the bowl inside the furnace is shown in Fig. 2.

Nitriding was performed inside an electric furnace for 3, 5 and 7 hours and the temperatures of the treatment were varied at 500°, 550°, and 600°C. Each specimen was named based on a combination of its variations, as shown in table 1.

Consequently, the specimens were taken out and cooled in the open air. Fig. 3 shows the pack nitrided specimens.

Table 1. Nomenclature of specimen

		Temperature (°C)		
		500	550	600
Time (h)	3	T500W3	T550W3	T600W3
	5	T500W5	T550W5	T600W5
	7	T500W7	T550W7	T600W7

Fig. 3: AISI 304 after treatment

2.3 Microvickers hardness test

According to ASTM E 384-17, a micro Vickers hardness test was performed using a Highwood HWMMT X7 machine, as shown in Fig. 4a. Furthermore, the load was set at 200gf for a 10 second dwell time and hardness was observed on several random spots. Each spot was indented at 18 sections, which were 0 to 150µm from the surface. The depth of the nitrided layer was measured using ISO 18203:2016 as guidelines[21]. The measurement started from the surface to a certain point where the hardness was 50 VHN greater than the core material. Prior to that, the top surface of each specimen was cut 5µm thick in order to observe its inner side (n = 7). Furthermore, specimens with the lowest, optimum, and highest hardness was also observed by SEM-EDS to know the microstructural and elemental transformation. The hardness was compared with commercial prosthesis materials (AISI 316L, CoCrMo alloy, Ti6Al4V alloy) and healthy human bone.

2.4 SEM-EDS observation

The depth of nitrogen penetration inside the specimens was observed using Scanning Electron Microscopy. Furthermore, Energy Dispersive X-Ray Spectroscopy was conducted to investigate the percentage of elements embodied in each specimen, especially N. A SEM-EDS observation was carried out using a Hitachi Flexsem 1,000 machine at the SEM Laboratory of the Mechanical Engineering Department, ITS Surabaya.

3. Results and discussions

3.1 Surface and composition analysis

3.1.1 SEM observation

According to the SEM observation, the thickness of the nitride layer became greater as the temperature and duration of the nitriding process increased. Furthermore, no nitride layer was formed on the untreated specimens, because no nitrogen percentage was detected.

T500W3 specimen in the cross-section, as observed by SEM, are shown in Figs. 4(a) to (b). Furthermore, pack nitriding on 500°C for 3 hours was able to form a 1.57 to 1.77µm thick nitride layer. Such depth was caused by the treatment that had been terminated before nitrogen atoms diffused on the deeper layer.

Cross-sectioned T550W7 specimens are shown in Figs. 4(c) to (d). 28.24 to 28.84µm thick compound zone was formed on the specimen. Furthermore, the thickness was increased, compared to the previous specimen which prompted an increased temperature and duration of treatment.

The nitrogen atoms were increased in order for them to diffuse deeper interstitially, resulting in more γ'-Fe_4N and CrN/Cr_2N phases formed. The lighter area close to the surface was rich in γ'-Fe_4N. Meanwhile, the presence of dark areas consist of chrome-nitride in the diffusion zone which proves the interaction between diffused N and Cr atoms[22].

In Figs. 4(e) to (f), SEM images of T600W7 specimen in cross-section were demonstrated. Furthermore, the deepest compound zone formed in this study, 50.3 to 50.63µm, was exhibited from treatment at 600ºC for 7 hours.

The rise of nitriding temperature prolonged the distance between compound atoms in order for easy interstitial diffusion of nitrogen into the iron atoms[23].

3.1.2 EDS observation

Figure 5 shows the untreated EDS, T500W3, T550W7, and T600W7 specimens. The most strategic areas to be observed were those closer to the surface, which had the highest number of N atoms detected[24]. Furthermore, no N atoms were detected on untreated specimens. Pack nitriding at 500ºC for 3 hours could diffuse 3.32 at %N atoms. 7.14 at %N atoms were detected on specimen treated at 550ºC for 7 hours. While the highest percentage of N atoms, 15.35 at % was detected on the T600W7 specimen. According to the data, it could be inferred that the N atoms that diffused into the specimens were more abundant when the treatment continued at higher temperatures and for a longer time.

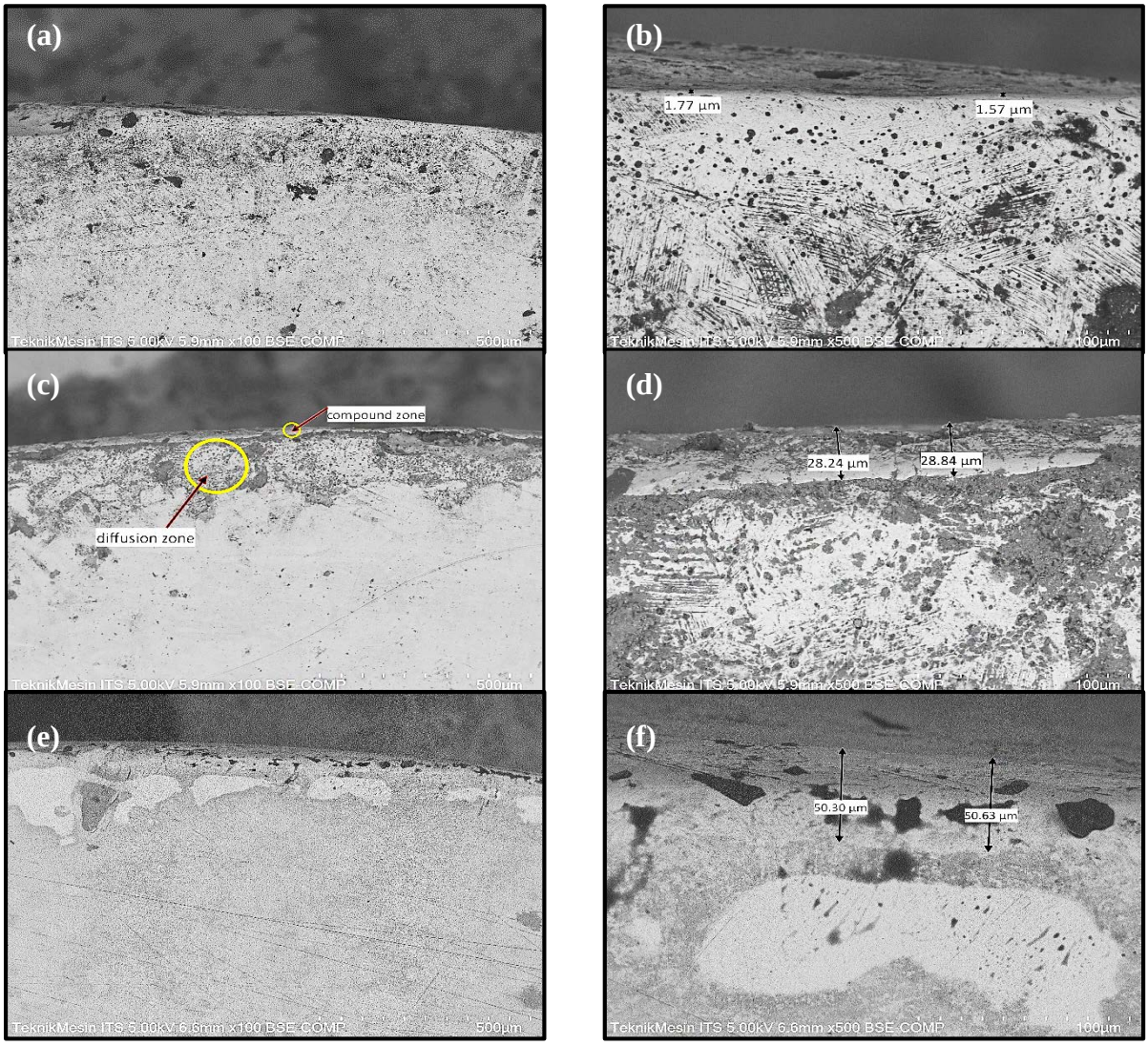

Fig. 4: (a), (b) SEM cross-section image of T500W3
(c), (d) SEM cross-section image of T550W7
(e), (f) SEM cross-section image of T600W7

Referring to the Fe-N phase diagram, γ and γ'-Fe_4N had already been formed at 600°C temperature and 15.35 at % N atoms. γ'-Fe_4N would be formed completely at an atomic percentage of 19.3 to 20%. Therefore, pack nitriding at 600°C for 7 hours, with a percentage of 40% urea weight, was unable to form a maximum γ'-Fe_4N phase.

Table 2 shows the percentage of Cr element against the time and temperature of the nitriding escalation. The decrease in the percentage of Cr content was due to the formation of nitride/carbide deposits. Furthermore, Lee[25] stated that it could destruct the passive layer (Cr_2O_3). The inhibited formation of the Cr_2O_3 layer resulted in a decrease in the capacity of the metal to resist corrosion. Therefore, the sensitization effect needs to be considered while deciding temperature and time variations.

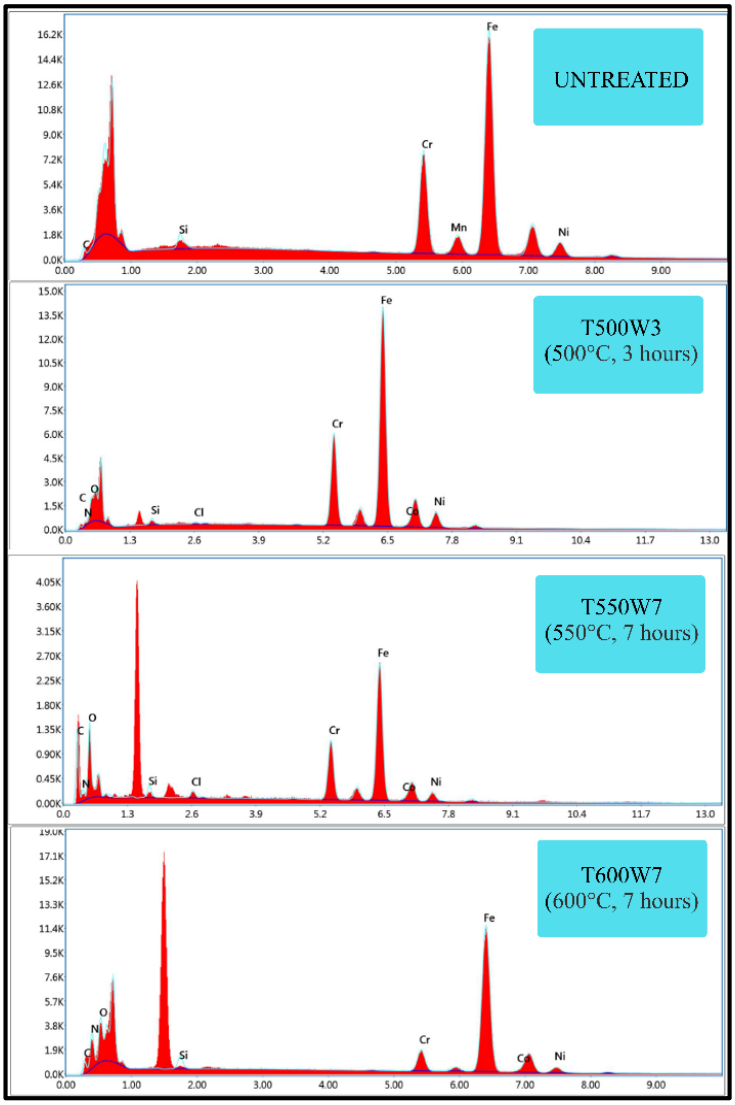

Fig. 5: EDS results on nitrided and untreated specimens

Table 2. Percentage of elements detected by EDS.

Elements	Specimen			
wt.% (at.%)	Untreated	T500W3	T550W7	T600W7
N	-	0,94 (3,32)	4,06 (7,14)	5,24 (15,35)
Cr	19,87 (19,35)	19,03 (18,02)	12,16 (5,76)	6,38 (5,04)
Fe	69,52 (65,13)	66,48 (60,4)	42,26 (18,64)	75,04 (55,15)
Ni	7,15 (6,38)	6,87 (5,76)	3,76 (1,58)	4,48 (3,13)

3.2 Microvickers hardness test

3.2.1 Surface hardness

Before microvickers test on the untreated specimen was carried out, the initial hardness of AISI 304 was 250.43 VHN. Therefore, the highest and lowest hardness of all specimens surpassed it, and was higher compared to healthy human bone (129 VHN). This means the specimens made by pack nitriding in this study are a safe alternative material for use in a hip joint prosthesis.

The phenomenon of increasing hardness as treatment duration lengthened as shown in Fig. 6 was similar with the existing theories. An increase in hardness was caused by a longer nitriding time that impacted more nitrogen atoms diffused on the modified layer[26-27]. Therefore, the longer the nitriding time, the denser the nitrogen concentration on the compound layer would be. It distorted the compound atoms' lattice parameter, which resulted in a harder specimens[28]. Moreover, nitrogen atoms would diffuse deeper when the treatment period is extended[29]. Hardness increase per two hours at 500°C was the lowest compared to 550°C and 600°C, which were 52.86 and 125.74 VHN respectively. Specimens nitrided at 550°C exhibited the highest jump, from 412.21 to 853.09 VHN at 5 to 7 hours. Furthermore, the hardness increase at 600°C was 400 VHN per two hours and reached a peak of 1,246.3 VHN by nitriding at 7 hours and 600°C.

Fig. 7 represents the hardness escalation as temperature increases. The lowest hardness rise was at 3 hours nitriding compared to 5 and 7 hours variation. Hardness increased to 36.11 VHN on the T500W5-T550W5 specimen, then escalated significantly on the T600W5 which was 376.74 VHN. This indicates that nitriding started to run effectively at 600°C. Furthermore, uniform hardness escalation of 350 VHN was observed on the time variation of 7 hours that could be proven through a stable increase along the T500W7-T550W7 to T600W7 line in Figure 6.

The value of hardness on Fig. 7 appeared to increase as temperature was rising on the constant time variation. Furthermore, nitrogen diffusion was faster at higher nitriding temperature[30]. Temperature rise broadens the distance between compound atoms in order for nitrogen atoms to diffuse between iron atoms more easily[23]. The partial pressure of N_2 gas gathered inside the bowl was smaller at lower nitriding temperatures. This lead to slower diffusion of nitrogen atoms through the surface, which resulted in a thin modified layer[31].

3.2.2 Hardness profile curve

The hardness curve was formed by the results of microhardness tests performed at 0 to 150µm. The nitriding hard depth (NHD) measurement was carried out according to DIN 50190-3 or ISO 18203:2016 standards. Depth measurement started from the surface to the distance where the hardness is 50 HVN greater than the substrate. Furthermore, the NHD point would be located at the intersection of the NHD line and the hardness curve.

The exact location could be pointed precisely by calculating the inverse ratio interpolation of the NHD

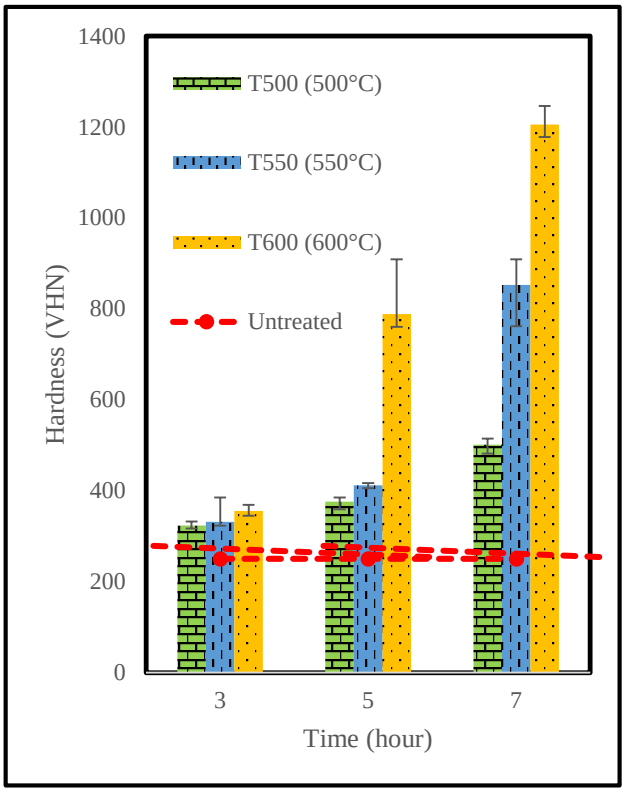

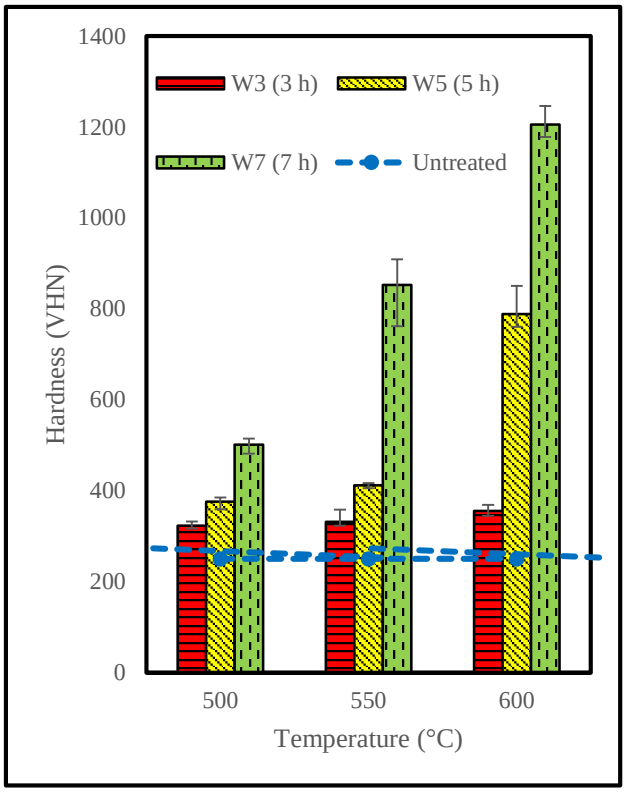

Fig. 6: (Left) Surface hardness of nitrided and untreated specimens as a function of temperature
Fig. 7: (Right) Surface hardness of nitrided and untreated specimens as a function of holding time

hardness and two nearest hardness points. Based on the standards mentioned and the initial hardness of AISI 304, it was concluded that the NHD limit for this research is 300.43 VHN.

Fig. 8(a) represents the influence of nitriding time on nitrogen penetration depth which is shown through the hardness curve. The hardness value at the beginning of the curve tends to be flat, and its value is insufficient for surface hardness. Subsequently, the curve declines until it slopes and approaches the initial hardness. The smaller nitrogen percentage diffused on greater depths caused the gradual drop. Furthermore, the high hardness at the beginning of the curve indicates the formation of new phases in the surface[31].

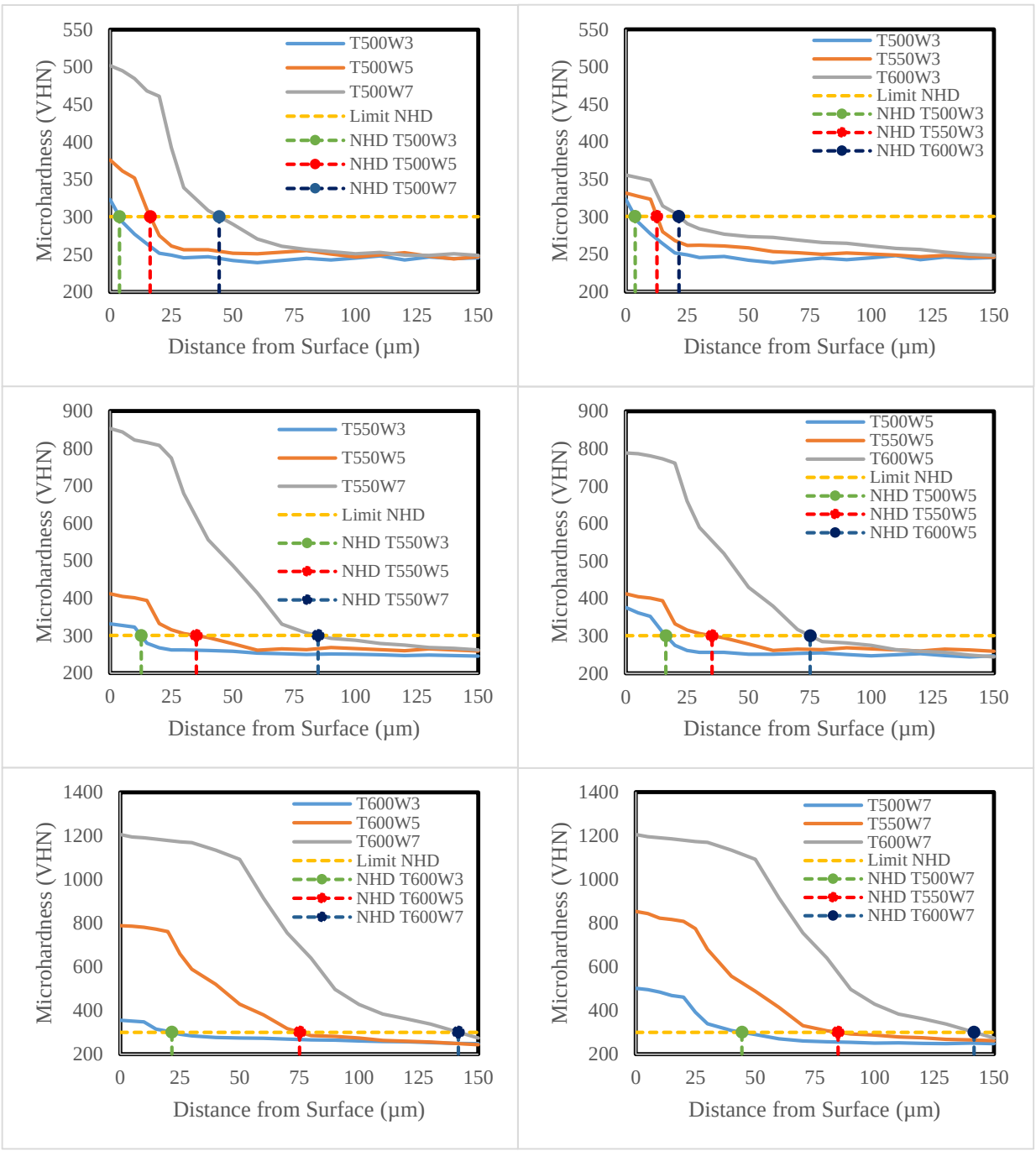

(a) (b)

Fig. 8: (a) Hardness profile of nitrided and untreated specimens as a function of holding time
(b) Hardness profile of nitrided and untreated specimens as a function of temperature

A hardness curve of 3 hours at 500°C declined from the start, indicating no compound zone and was formed at a distance of 0 to 5µm. Furthermore, the specimen nitrided for 5 hours at 500°C peak in hardness from the surface until 10µm. The starting curve of the nitrided specimen involving a 7-hour timing at 500°C remained high until 20µm, which was more than the previous specimens. Therefore, it was concluded that pack nitriding performed at 500°C did not exhibit optimal results at 3 and 5-hour timings.

At the beginning of the curve, specimens nitrided at 550°C appeared more stable compared to those at 500°C. The hardness curve of 3 and 5-hours duration began to decline at an adjacent distance, which was 15µm and 20µm. Furthermore, a notable distinction was evident for 7 hours duration at 550°C and the curve started to flatten at 90µm after sloping from 25µm. Nitriding at 550°C occurred more effectively than with the 500°C variation, especially over 7 hours and each of the 600°C hardness profiles displayed unique features.

The 3-hour profile reached its highest at 0 to 10µm, then sloped and started to approach substrate hardness at 50µm. At the surface up to 20µm deep, the 5-hour profile remained high and stable and the 7-hour profile showed the deepest nitrided layer, 40 µm. Furthermore, at 90 to 100µm, the 7-hour curve had already sloped, but the value ranging between 230 to 280 VHN, was not yet close to the untreated specimen.

The impact of nitriding temperature on nitrogen penetration depth is shown in Fig. 8(b) as hardness curves. Based on the curves, each hardness measurement peaks at the surface decreases gradually until it approaches the untreated specimen value[32].

The 500° and 550°C specimens nitrided for 3 hours sloped at the same distance, namely 550 µm. In the initial stage, the 550° and 600°C curves appeared to remain stable at the same distance, which was 10µm. However, the 600°C specimen contained higher hardness and started to slope at the further distance, which was 70µm.

The dissimilarity between the three curves of 5-hour duration was more remarkable in the 600°C specimen in contrast to those at 500° and 550°C. Beginning with a surface hardness that was twice as large as the slope, the curve's early stage was flat until 20µm. After that, it declined to 80µm before starting to slope onwards.

The hardness curve of the specimens that were treated for 7 hours at 500°, 550°, and 600°C also displayed unique characteristics. The specimen at 500°C was the highest at the surface until 20µm, then it decreased and sloped at 60µm. In addition, the specimen at 550°C was the highest and stable at a distance of 0 to 25µm, and later declined and sloped at 90µm. The deepest nitrogen penetration was found on the 600°C variation (50 µm).

Based on the test results, the core hardness of AISI 304 was 250.43 VHN. Therefore, the limit of hard-depth of nitriding (NHD) is 300.43 VHN. Table 3 shows the increase in layer thickness formed by increasing time and temperature. Furthermore, the mobility of the nitrogen atom slows at low temperatures[33] and the nitride layer formed in the specimen at high temperatures becomes thicker.

Table 3. Nitriding hard depth (NHD) on µm

		Temperature (°C)		
		500	550	600
Time (h)	3	3,77	16,35	44,43
	5	12,64	35,11	84,71
	7	21,61	75,14	141,64

3.3 Hardness comparison

This was carried out to analyze the capability of pack nitrided AISI 304 as an alternative to commercial hip joint implant materials. Those materials include AISI 316L, CoCrMo, and Ti6Al4V alloy. Furthermore, the hardness was also compared to healthy human bone. This comparison is shown in Fig. 14.

Figure 9 shows that the pack nitriding process carried out in this study had the highest hardness at 600ºC and with 7 hours of treatment (1205.87 VHN). Furthermore, its value was higher than other treatments (250.43 and 412.21 VHN). This value was also higher than the hardness in AISI 316L (316.1 VHN), Ti6Al4V (435.7 VHN), CoCrMo (351 VHN), and healthy human bones (129 VHN). Therefore, these results show that pack nitrided AISI 304 is a possible alternative material for hip joint prostheses when determined by the hardness aspect. The specimen treated at 550°C for 5 hours proved the best choice since its hardness fit into the range of materials in general use.

Fabrication of pack-nitrided AISI 304 requires more frugal equipment than other types of nitriding, especially plasma and liquid. Through varying treatment temperatures and duration, hardness value could be tailored to the needs of the biomaterial industry. Despite its advantages, pack nitrided AISI 304 also has disadvantages as an implant material. Furthermore, the nitrided specimen would lack protection from corrosion because nitriding tends to strip down the passive layer. Xie et al. stated that the low-pressure nitriding process has been applied to the AISI 304. The result showed that a nitrided layer with a high surface and smooth hardness gradient could be obtained by low-pressure gas nitriding, which contributed to improving the toughness. Another result was the low-pressure nitrided layer which presented a lower anodic corrosion current when compared to that of the atmospheric pressure and indicated a better corrosion resistance[34]

Lie et al., stated that nitriding treatments have been successfully applied to austenitic stainless steels to improve their hardness and tribological properties. However, at temperatures above 450 °C, conventional plasma nitriding processes decrease the corrosion

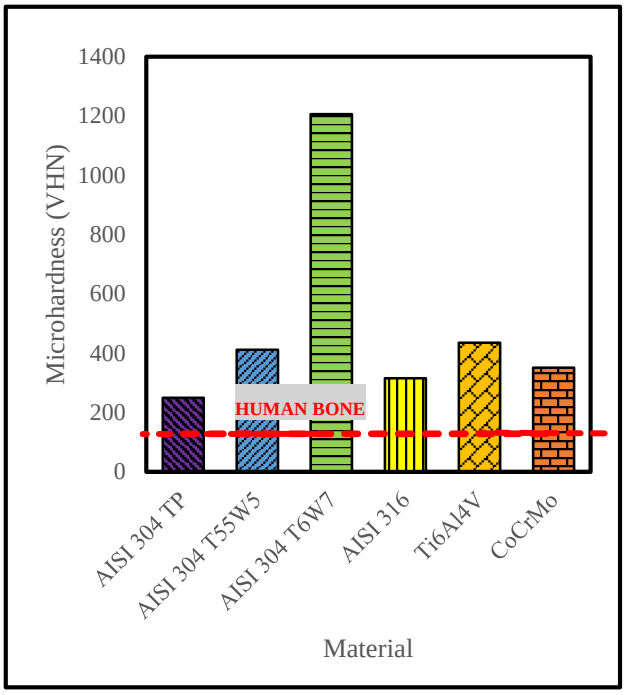

Fig. 9: Hardness of specimens compared to commercial hip joint prosthesis material and healthy human bone

resistance due to the formation of CrN phases within the modified layer[35].

4. Conclusions

Pack nitriding as a method to enhance the hardness and microstructure of AISI 304 was proposed in this study.

- The hardness of AISI 304 depends on the temperature and duration of pack nitriding.
- Nitrogen was found on pack nitrided AISI 304. Furthermore, Fe and Cr, as main components of the specimen, reacted with diffused N. At an N-atomic percentage of 15.35%, γ'-Fe_4N phase was already formed. However, γ'-Fe_4N formed by pack nitriding using a 40 wt.% N nitriding agent had not yet exceeded the optimum result due to the nitrogen atoms diffusion not exceeding the range of 19.3 to 20%.
- The advantages of pack nitrided AISI 304 as a material for prostheses include the much simpler manufacturing process and the ease of output (hardness) control. Meanwhile, the key drawback is the lack of protection from corrosion. In addition, AISI 304 treated at 550°C for 5 hours is recommended as an alternative material for artificial hip joints.

Acknowledgements

The authors acknowledge the support of Department of Mechanical Engineering UNS via PTUPT research grant 2019 DGHE Ministry of Education and Culture Republic of Indonesia no: 092/SP2H/LT/DRPM/2019.

References

1) Moses Kamita, Mitsuru Shindo, Arihiro Kano, Macrophage Colony-Stimulating Factor mediates its Immunosuppressive Activity through the Emerging Myeloid Cells during Tumor Progression, EVERGREEN Joint Journal of Novel Carbon Resource Sciences & Green Asia Strategy, Vol. 04, Issue 02/03, pp. 18 -22, September 2017
2) H. Yuliantini, Education on Dislocation Prevention and Supervised In-Hospital Exercise Program for Post Total Hip Arthroplasty Clients in the Surgery Room of the Middle Right Orchid Class, RSUP Persahabatan, Universitas Indonesia, Depok, 2013.
3) S. Ghosh, S. Abanteriba, Status of surface modification techniques for artificial hip implants, Sci. Technol. Adv. Mater. 17 (2016) 715–735. https://doi.org/10.1080/14686996.2016.1240575.
4) M.A. Elloy, J.T.M. Wright, M.E. Cavendish, The Basic Requirements and Design Criteria for Total Joint Prostheses, Acta Orthop. Scand. 47 (1976) 193–202. https://doi.org/10.3109/17453677608989718.
5) P.W. Grieco, S. Pascal, J.M. Newman, N. V. Shah, S.G. Stroud, N.P. Sheth, A. V. Maheshwari, New alternate bearing surfaces in total hip arthroplasty: A review of the current literature, J. Clin. Orthop. Trauma. 9 (2018) 7–16. https://doi.org/10.1016/j.jcot.2017.10.013.
6) M.B. Nasab, M.R. Hassan, Metallic Biomaterials of Knee and Hip-A Review, Trends Biomater. Artif. Organs. 24 (2010) 69–82. http://www.biomedsearch.com/article/Metallic-biomaterials-knee-hip-review/308129449.html%0Apapers3://publication/uuid/567DB2D7-F6E2-4F94-880C-13044E1FFF75%0Apapers3://publication/uuid/FF6A0550-652C-4DF6-B049-26FFF5EF2803.
7) J. Alvarado, R. Maldonado, J. Marxuach, R. Otero, Biomechanics of Hip and Knee Prostheses, Engineering. (2003) 1–20.
8) Shailendra Singh Chauhan, S C Bhaduri, Structural analysis of a Four-bar linkage mechanism of Prosthetic knee joint using Finite Element Method, EVERGREEN Joint Journal of Novel Carbon Resource Sciences & Green Asia Strategy, Vol. 07, Issue 02, pp209-215, June, 2020.
9) Abdullah, Abdul Halim, Todo, Mitsugu, Effects of Total Hip Arthroplasty on Stress Adaptation and Bone Remodeling in Lower Limbs, EVERGREEN Joint Journal of Novel Carbon Resource Sciences & Green Asia Strategy, Vol. 02, Issue 01, pp. 6-11, March 2015.
10) Mehak Sharma, Manoj Soni, A musculoskeletal Finite Element Study of a Unique and Customised Jaw Joint Prosthesis for the Asian Populace, EVERGREENJoint Journal of Novel Carbon Resource Sciences & Green Asia Strategy, Vol. 07, Issue 03,pp351-358, September, 2020
11) US Food and Drug Administration, Concerns about

Metal-on-Metal Hip Implants Metal on Metal Hip Implants Outside of the United States, (2019) 1–3. https://www.fda.gov/medical-devices/metal-metal-hip-implants/concerns-about-metal-metal-hip-implants.
12) Y. Lin, W. Lan, K. Ou, C. Liu, P. Peng, Surface & Coatings Technology Hemocompatibility evaluation of plasma-nitrided austenitic stainless steels at low temperature, Surf. Coat. Technol. 206 (2012) 4785–4790. https://doi.org/10.1016/j.surfcoat.2012.03.089.
13) Z.A. Uwais, M.A. Hussein, M.A. Samad, N. Al-Aqeeli, Surface Modification of Metallic Biomaterials for Better Tribological Properties: A Review, Arab. J. Sci. Eng. 42 (2017) 4493–4512. https://doi.org/10.1007/s13369-017-2624-x.
14) H. Hermawan, Introduction to Biomaterial, (2019) 1–8. https://doi.org/10.31227/osf.io/v3z5t.1/8.
15) Yos Phanny, Mitsugu Todo, Effect of Sintering Time on Microstructure and Mechanical Properties of Hydroxyapatite Porous Materials for Bone Tissue Engineering Application, EVERGREEN Joint Journal of Novel Carbon Resource Sciences & Green Asia Strategy, Vol. 01, Issue 02, pp. 1-4, September 2014
16) L. Kunčická, R. Kocich, T.C. Lowe, Advances in metals and alloys for joint replacement, Prog. Mater. Sci. 88 (2017) 232–280. https://doi.org/10.1016/j.pmatsci.2017.04.002.
17) Lutfiyatul Mukhlisah, Barlah Rumhayati, Modification of Biochitin Immobilized Dithizone as Adsorbent for Cr (VI) Removal, EVERGREEN Joint Journal of Novel Carbon Resource Sciences & Green Asia Strategy, Vol. 07, Issue 03, pp429-435, September, 2020
18) Elviyenti, Effect of Nitriding on Corrosion Rate of AISI 316L Stainless Steel with Pack Nitriding Method, Universitas Andalas, 2010.
19) F.H. Bakran, Effect of Nitriding on Corrosion Rate in Steel KS01, Bogor Agricultural University, 2011.
20) ASTM Standard, Standard Test Method for Microindentation Hardness of Materials, ASTM International, West Conshohocken, PA, 2017. https://doi.org/10.1520/E0384-17.
21) D. Kovács, I. Quintana, J. Dobránszky, Effects of Different Variants of Plasma Nitriding on the Properties of the Nitrided Layer, J. Mater. Eng. Perform. 28 (2019) 5485–5493. https://doi.org/10.1007/s11665-019-04292-9.
22) Badrulzzaman, Nitriding of AISI 316L Austenitic Stainless Steel at Low Temperature for the Enhancement of Surface Properties and Corrosion Properties, Universiti Teknologi Petronas, 2013.
23) R. Kartikasari, I. Aziz, Corrosion Behavior of Plasma Nitrided SS316L Biomaterial Abstract :, (2017) 29–37. https://doi.org/10.2174/1874088X01711010029.
24) F. Borgioli, From austenitic stainless steel to expanded austenite-s phase: Formation, characteristics and properties of an elusive metastable phase, Metals (Basel). 10 (2020). https://doi.org/10.3390/met10020187.
25) I. Lee, Effect of processing temperatures on characteristics of surface layers of low temperature plasma nitrocarburized AISI 204Cu austenitic stainless steel, Trans. Nonferrous Met. Soc. China. 22 (2012) s678–s682. https://doi.org/10.1016/S1003-6326(12)61785-3.
26) H. Göhring, O. Fabrichnaya, A. Leineweber, E.J. Mittemeijer, Thermodynamics of the Fe-N and Fe-N-C Systems: The Fe-N and Fe-N-C Phase Diagrams Revisited, Metall. Mater. Trans. A Phys. Metall. Mater. Sci. 47 (2016) 6173–6186
27) A. Triwiyanto, P. Hussain, A. Rahman, M.C. Ismail, The Influence of Nitriding Time of AISI 316L Stainless Steel on Microstructure and Tribological Properties, Asian J. Sci. Res. 6 (2013) 323–330. https://doi.org/10.3923/ajsr.2013.323.330.
28) A.F. Yetim, F. Yildiz, A. Alsaran, A. çelik, Surface modification of 316L stainless steel with plasma nitriding, 2008.
29) S. Rahayu, N. Setiawan, S. Virdhian, E. Suhendi, Effect of Powder Nitriding Process on Changes in Hardness and Thickness of Diffusion Layer on High Speed Steel Lathe Chisels, Met. Indones. 39 (2017).
30) A.B. Setiawan, W. Purwadi, Effect of Temperature and Time of Nitriding Process on Surface Hardness of FCD 700 with Urea Nitriding Media, (2009) 35–40.
31) K.Y. Li, Z.D. Xiang, Increasing surface hardness of austenitic stainless steels by pack nitriding process, Surf. Coatings Technol. 204 (2010) 2268–2272. https://doi.org/10.1016/j.surfcoat.2009.12.022.
32) N.Z.S. Affandi, The Effective Duration of Gas Nitriding Process of AISI 316L, Universiti Teknologi Petronas, 2013.
33) A. Turk, C. Bindal, Characterization of plasma nitrided X32CrMoV33 die steel, Mater. Manuf. Process. 24 (2009) 898–902. https://doi.org/10.1080/10426910902844278.
34) Xie W., Chen Y., Chen D., Yang Y., Zhang C., Cui G.,and Wang Y., Low-pressure gas nitriding of AISI 304 austenitic stainless steel: reducing the precipitation of chromium nitrides, Material Research Express 7 (2020) 066406 https://doi.org/10.1088/2053-1591/ab9bef
35) Li Y., He Y., Zhang S., Wang W., Zhu Y., Microstructure and corrosion resistance of nitrogen-rich surface layers on AISI 304 stainless steel by rapid nitriding in a hollow cathode discharge, Applied Physics A (2018) 124:65 https://doi.org/10.1007/s00339-017-1499-8